Synergic effect in gelation by two-component mixture of chiral gelators†

Zoran Džolić,[a] Kristina Wolsperger[b] and Mladen Žinić*[a]

Received (in Montpellier, France) 6th July 2006, Accepted 31st August 2006
First published as an Advance Article on the web 12th September 2006
DOI: 10.1039/b609642e

Observation of the synergic gelation effect (SGE) in two-component gels is reported. An equimolar mixture of (*S*,*S*)-bis(LeuOH) oxalamide [(*S*,*S*)-**1**] and (*S*,*S*)-bis(leucinol) oxalamide [(*S*,*S*)-**2**] is able to gel up to 7 times larger a volume of *p*-xylene than an equal mass of each component and up to 5 times larger a volume than an equal mass of the (*S*,*S*)-**1** + (*R*,*R*)-**2** or (*S*,*S*)-**1** + *rac*-**2** equimolar mixtures. The homochiral (*S*,*S*)-**1** + (*S*,*S*)-**2** combination of gelators is capable of hardening a volumes up to 5 times larger of certain solvents than the heterochiral (*S*,*S*)-**1** + (*R*,*R*)-**2** combination. Experimental evidence provided by determination of gelation efficiency, by ^{1}H NMR, TEM and XRD studies, by determination of phase transition diagrams and calculations of thermodynamic parameters for gel melting processes shows that synergism depends on the chirality of the components, on the solvent properties and on the gel morphology. It was found that each component tends to form reversed bilayers in lipophilic solvents which then interact and organize into gel unit fibers. The unit fibers formed by interaction of the (*S*,*S*)-**1** and (*S*,*S*)-**2** bilayers and of the (*S*,*S*)-**1** and (*R*,*R*)-**2** bilayers are distereoisomeric. In certain solvents, such diastereomeric unit fibers give different gel morphologies which in turn results by different thermal stabilities of the gels, and in some cases by dramatically different gelling efficiencies of gelator mixtures. The latter observation is denoted as the synergic gelation effect (SGE).

Introduction

The gelation of various fluids by low molecular weight organic compounds represents a topic of fast increasing interest.[1] Numerous applications of gels as "smart" soft materials are possible, relying on the controlled gel-to-sol phase transition, which can be triggered by various external or internal stimuli such as temperature, light, pH or recognition of a specific solute.[2–6] Applications include new drug delivery systems,[7] tissue engineering,[8] treatment of fluid waste[9] and, more recently, preparation of nano-dimensional inorganic materials by sol–gel processes.[10,11] It has been shown that gels form by the self-assembly of gelator molecules into fibrous aggregates through highly specific intermolecular interactions.[12–14] When the aggregates are sufficiently long, they entangle into a three-dimensional network capable of immobilizing the solvent.[15–19] The most recent interest is directed toward the development of two-component gelling systems based on constitutionally different non-gelling molecules capable of gelling upon mixing.[20] Such two-component gels endow supramolecular systems of higher level of complexity and hence open new ways of control and modulation of gel properties or phase transition processes.

We have recently found that bis(amino acid) **1** and bis(amino alcohol) oxalamides **2** are efficient gelators of various organic solvents and water.[21] Both types of gelators tend to self-assemble by forming β-networks of cooperative hydrogen bonds between oxalamide units in one direction and between terminal carboxylic or hydroxyl groups in the second in-plane direction. The lipophilic amino acid groups and the polar terminal groups (COOH or OH) are located above and below the oxalamide plane, respectively. Such separation of lipophilic and polar groups leads to a bilayer type of organization in the third dimension (Fig. 1).[21a,c]

Since both types of structurally closely related gelators exhibit the same type of self-assembly, the following questions could be raised: (1) could gels form by mixing two constitutionally different gelators; (2) would the properties of two-component gels be different from those formed by the single components; (3) if gels were formed do the gelator molecules form composite assemblies, and if so, would they form hybrid bilayers consisting of both components or composite assemblies consisting of interacting single-component bilayers; (4) what would be the role of chirality in such two-component systems? If the gels containing composite assemblies of the constitutionally different gelator molecules could form, this would present the supramolecular (non-covalent) variant of molecular (covalent) copolymerization and may give gels of considerably different properties than those formed by each single component. In such a case, new and more complex gelation systems could be obtained opening new ways of control of the properties or phase transitions, which in turn

[a] *Department of Organic Chemistry and Biochemistry, Laboratory of Supramolecular and Nucleoside Chemistry, Ruđer Bošković Institute, Bijenička 54, 10 000 Zagreb, Croatia. E-mail: zinic@irb.hr; Fax: +385 1 46 80 195; Tel: +385 1 46 80 217*
[b] *NMR Center, Ruđer Bošković Institute, Bijenička 54, 10 000 Zagreb, Croatia*

† Electronic supplementary information (ESI) available: T_{gel} as function of the molar ratio of (*S*,*S*)-**1** to (*R*,*R*)-**2** in *p*-xylene gels, TEM images of toluene and *p*-xylene gels of components, temperature–dissolution profiles for *o*-xylene-d_{10} gel samples, temperature-dependent ^{1}H NMR spectra of *o*-xylene-d_{10} gel of (*S*,*S*)-**1** + *rac*-**2**, and minimized conformation of (*S*,*S*)-**1**. See DOI: 10.1039/b609642e

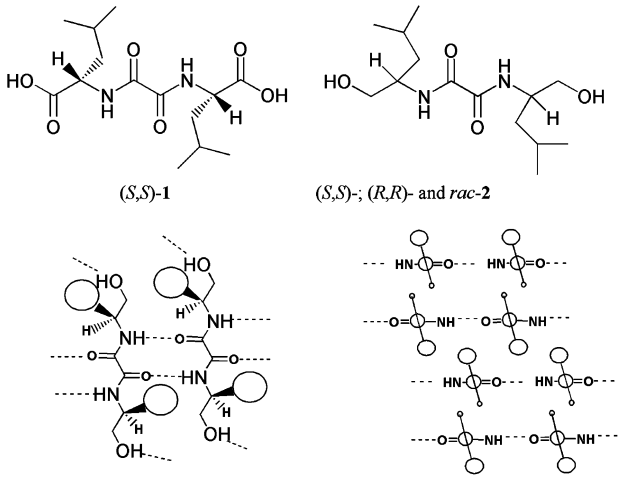

Fig. 1 Structures of **1** and **2** and the organization of gel assemblies by the hydrogen bonding network (left; shown for **2**) and lipophilic and polar interactions (right) between *i*-Bu (large circles) and OH or COOH groups (small circles), respectively, in reversed bilayers formed in lipophilic solvents.

may result in various new applications as dynamic and controllable soft materials.

In this work we report on the discovery of a synergic gelation effect (SGE) showing that the defined mass of the homochiral 1 : 1 molar mixture of constitutionally different gelators **1** and **2** is capable of gelling impressively larger volumes of certain solvents than an equal mass of each of the components or an equal mass of the heterochiral mixture. Results of systematic studies of synergic and non-synergic two-component gels by TEM, ^{1}H NMR and X-ray powder diffraction (XRPD), together with thermodynamic parameters determined from their phase transition diagrams, reveal that the observed synergic phenomenon is clearly solvent and chirality dependent, and that it originates from a diastereomeric relationship between gel assemblies, which form by interaction of reversed bilayers of the components, and that is finally expressed in different gel morphologies.

Results and discussion

Gelation experiments—the synergism

To investigate if two-component gels could form from **1** and **2**, we prepared 1 : 1 molar mixtures of the (*S*,*S*)-bis(LeuOH) derivative **1** with each of the enantiomers of bis(leucinol) oxalamide (*S*,*S*-**2** and *R*,*R*-**2**) and also with its racemate (*rac*-**2**). Gelation capacity of each of the components and their mixtures was assessed against five aromatic solvents using in each test an identical weighted amount of pure gelator or a 1 : 1 molar mixture of the components (Table 1).

Among the three mixtures, the (*S*,*S*)-**1** + (*S*,*S*)-**2** two-component system is capable of immobilizing impressively larger volumes of *p*-xylene, *m*-xylene and toluene than the same amount of each single component or the heterochiral (*S*,*S*)-**1** + (*R*,*R*)-**2** and (*S*,*S*)-**1** + *rac*-**2** mixture.

For example, 1 mg of (*S*,*S*)-**1** + (*S*,*S*)-**2** is capable of gelling a 7 times larger volume of *p*-xylene than 1 mg of (*S*,*S*)-**1** and a 4 times larger volume than 1 mg of (*S*,*S*)-**2**; the example shows that mixing two constitutionally different gelators of the same chirality may result in an impressive increase in the gelation efficiency compared to that of each of the single components. However, 1 mg of (*S*,*S*)-**1** + (*S*,*S*)-**2** is also able to gel a 5 times larger volume of the same solvent than 1 mg of the heterochiral combination (*S*,*S*)-**1** + (*R*,*R*)-**2**, and more than 5 times larger volume than 1 mg of the (*S*,*S*)-**1** + *rac*-**2** mixture. These results show that SGE occurs only in the case of the homochiral combination of chiral components. Pronounced SGE's are observed in *p*-xylene, *m*-xylene and toluene (Table 1), however, they are only very slight in benzene and *o*-xylene. The gelation results from Table 1 clearly show that SGE is (a) solvent dependent, showing dramatic differences between the five aromatic solvents tested (compare *o*- and *p*-xylene), and (b) exhibited only by the homochiral combination of the components and not by the heterochiral and diastereomeric ones.

To determine whether interactions between (*S*,*S*)-**1** and (*S*,*S*)-**2** or (*R*,*R*)-**2** induce thermal stabilization of the two-component gel, the T_{gel} measurements with different ratios of the two gelators were carried out. In *p*-xylene the maximum T_{gel} was measured for a (*S*,*S*)-**1** : (*S*,*S*)-**2** 1 : 1 molar ratio showing a stabilization of 20–26 °C for the homochiral combination (Fig. 2) and, of 15–21 °C for the heterochiral (*S*,*S*)-**1**/(*R*,*R*)-**2** combination (Supp. Inf. Fig. 1†) compared to T_{gel} of the gels formed by the same concentration of the single components. These results clearly show that the interaction between the gelators **1** and **2** results in thermal stabilization of the two component gels.

TEM investigation

The gel formed by (*S*,*S*)-**1** + (*S*,*S*)-**2** in toluene at the maximal volume of gelled solvent (1.42 mL mg^{-1}, Table 1) gives the TEM image showing many tiny curved fibers with diameters in the range of 10–80 nm (Fig. 3a). However, the TEM image of

Table 1 Results of the gelation tests[a] for (*S*,*S*)-**1**, (*S*,*S*)-**2**[b] and *rac*-**2** and the 1 : 1 mixtures of **1** and **2**

Solvent	(*S*,*S*)-**1**	(*S*,*S*)-**2**	*rac*-**2**	(*S*,*S*)-**1** + (*S*,*S*)-**2**	(*S*,*S*)-**1** + (*R*,*R*)-**2**	(*S*,*S*)-**1** + *rac*-**2**
Toluene	0.28	0.50	1.50	1.42	0.48	0.28
Benzene	0.10	1.00	0.80	0.81	0.46	0.33
p-xylene	0.52	0.85	0.20	3.72	0.72	0.70
m-xylene	0.36	0.95	0.15	2.28	0.72	0.53
o-xylene	0.42	1.40	0.86	0.70	0.56	0.30

[a] Gelation efficiency expressed as mL of a solvent gelled by 1 mg of a single component or by 1 mg of a 1 : 1 molar mixture of the components. Gelation tests were performed in test tubes with 10 mm inner diameter. [b] (*R*,*R*)-**2** has the same gelation properties as (*S*,*S*)-**2**.

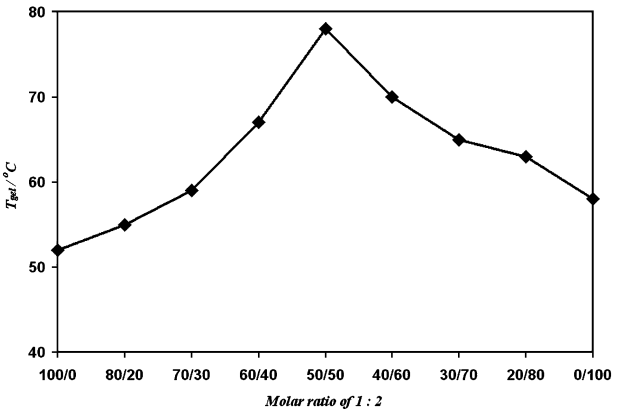

Fig. 2 T_{gel} as function of the molar ratio of (*S*,*S*)-**1** to (*S*,*S*)-**2** in *p*-xylene gels.

the (*S*,*S*)-**1** + (*R*,*R*)-**2** toluene gel also taken at the maximal volume of gelled toluene (0.48 mL mg^{-1}, Table 1) is completely different: the network consists of large fiber bundles (Fig. 3b).

Apparently, close to the minimal gelation concentrations the morphologies of the (*S*,*S*)-**1** + (*S*,*S*)-**2** and the (*S*,*S*)-**1** + (*R*,*R*)-**2** gels are different. The AFM images (Fig. 3c and d) taken on the same diluted gels also showed clearly different morphologies for the two systems: much thinner fibers for the homochiral combination and thick and straight fiber bundles for the heterochiral one were observed. Interestingly, the TEM image of the (*S*,*S*)-**1** + *rac*-**2** toluene gel also taken at the maximal volume of the solvent (0.28 mL mg^{-1}) represents a combination of the two former images showing the presence of two different morphologies, the tiny curved fibers and large fiber bundles. The TEM investigation explains the observed SGE in toluene. For the same quantity of the (*S*,*S*)-**1** + (*S*,*S*)-**2** and the (*S*,*S*)-**1** + (*R*,*R*)-**2** two-component mixture, the former gives much thinner fibers than the latter. Hence, the first mixture gives "more" fibers being capable of immobilizing a larger volume of toluene. In contrast, the (*S*,*S*)-**1** + (*R*,*R*)-**2** gives thick fiber bundles and is hence capable of hardening a smaller volume of toluene.

In the TEM images of (*S*,*S*)-**1** + (*S*,*S*)-**2** and (*S*,*S*)-**1** + (*R*,*R*)-**2** *p*- and *m*-xylene gels, also taken at maximal volumes of the solvents (Table 1), the same differences in morphology were also observed. The homochiral combinations exhibiting pronounced synergism give very dense gel networks consisting of thin fibers with diameters between 15 and 80 nm (Fig. 4a and c), while the heterochiral ones give many pronounced straight and thick fiber bundles having diameters in the range of 100–280 nm (Fig. 4b and d).

The *o*-xylene gels showing only slight SGE for the homochiral combination were also investigated by TEM. The Pd shadowed images of the (*S*,*S*)-**1** + (*S*,*S*)-**2** and (*S*,*S*)-**1** + (*R*,*R*)-**2** gels, both taken at the maximal volume of the solvent, show practically identical morphologies with many curved tiny fibers having in both cases diameters of around 20 nm (Fig. 5a and b).

The morphologies of the single component [(*S*,*S*)-**1** and (*S*,*S*)- and *rac*-**2**] toluene and *p*-xylene gels exhibit tiny curved fibers with diameters of 10–80 nm for the first component, and straight and thick fiber bundles with diameters of 50–180 nm

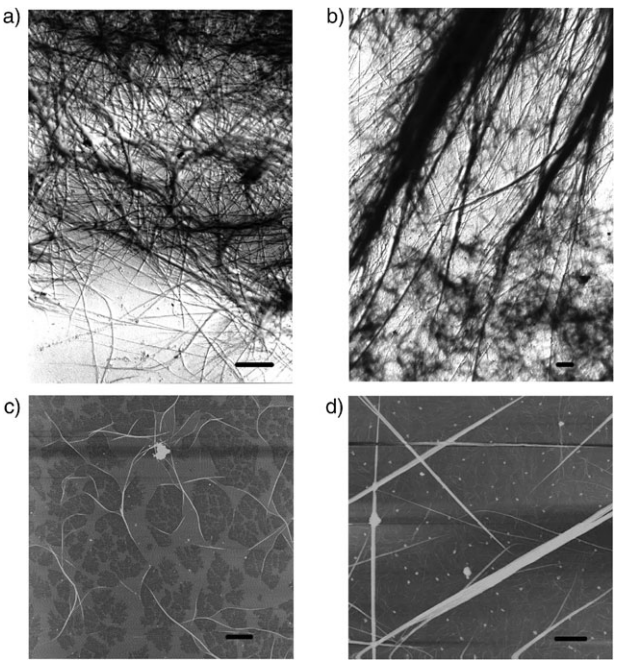

Fig. 3 TEM images of Pd shadowed (a) (*S*,*S*)-**1** + (*S*,*S*)-**2**; (b) (*S*,*S*)-**1** + (*R*,*R*)-**2**. AFM images of (c) (*S*,*S*)-**1** + (*S*,*S*)-**2** diluted gel, fiber heights 10–20 nm and (d) (*S*,*S*)-**1** + (*R*,*R*)-**2** diluted gel, fiber heights 26–143 nm (scale bars = 1 μm).

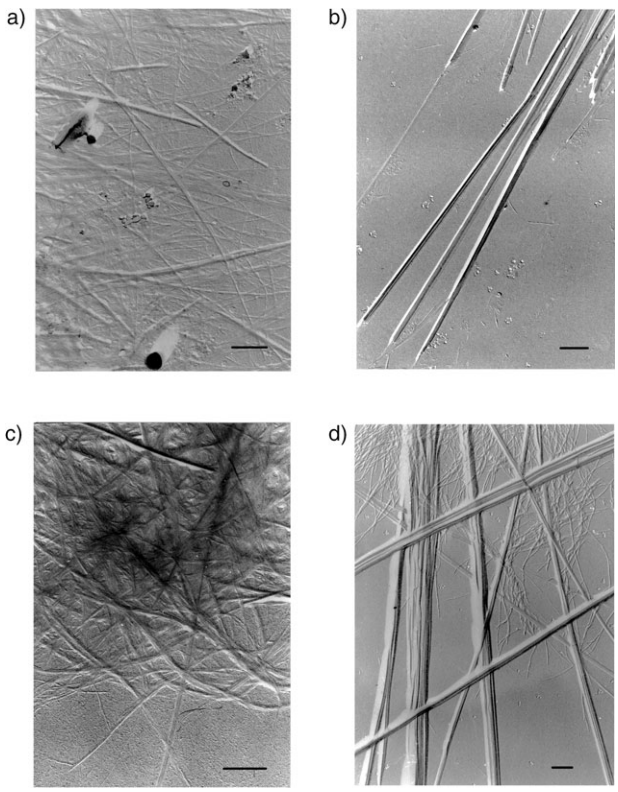

Fig. 4 TEM images of Pd shadowed (a) (*S*,*S*)-**1** + (*S*,*S*)-**2** *p*-xylene gel; (b) (*S*,*S*)-**1** + (*R*,*R*)-**2** *p*-xylene gel, (c) (*S*,*S*)-**1** + (*S*,*S*)-**2** *m*-xylene gel; (d) (*S*,*S*)-**1** + (*R*,*R*)-**2** *m*-xylene gel (scale bars = 0.5 μm).

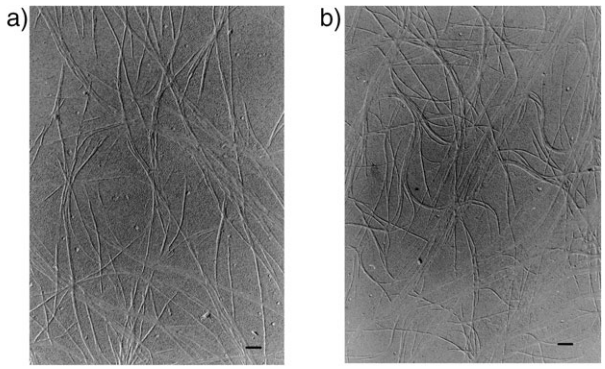

Fig. 5 TEM images of Pd shadowed (a) (*S,S*)-**1** + (*S,S*)-**2** and (b) (*S,S*)-**1** + (*R,R*)-**2** *o*-xylene gels (scale bars = 0.2 μm).

for the (*S,S*)- and *rac*-**2** (Supp. Inf. Fig. 2 and 3†). It should be noted that the morphologies observed for the homo- and hetero-chiral mixtures (Fig. 3–5) always show the presence of only one type of fiber, being either tiny curved ones or straight fiber bundles, and not the simultaneous presence of both fiber types. Hence, it can be concluded that in the two component gels the network consists of composite fibers and not of the independent fibers of each component.

TEM investigation also suggests that the SGE observed for the homochiral combination of **1** and **2** and lack of it for the heterochiral combination is a consequence of different gel morphologies in the two systems and that in *o*-xylene gels, where only very slight SGE is observed for the homochiral combination, both combinations practically give identical morphologies.

^{1}H NMR investigation

Heating of gel samples is known to result in an increase of gelator ^{1}H NMR signals due to disaggregation of the gel network into smaller, dissolvable aggregates observable by NMR.[21,22] To check the thermal behaviour of the toluene gels of the synergic, homochiral and the non-synergic, heterochiral gelator mixtures their temperature–dissolution profiles were determined.

Fig. 6a and b show the increase of **1** and **2** concentrations by heating (*S,S*)-**1** + (*S,S*)-**2** (a) and (*S,S*)-**1** + (*R,R*)-**2** (b) toluene gel samples (each containing known concentrations of 1,1,2,2-tetrachloroethane as an internal standard), as calculated from the increase of gelator signals (similar profiles of the *o*-xylene gels are included in the Supp. Inf. as Fig. 4†); the dissolution slopes (mmol °C^{-1}) determined for each component in the six gels are shown in Table 2.

The profiles show much better dissolution of the alcohol component with increasing temperature in all of the six gels examined. For the toluene gels, the component (*S,S*)-**2**, (*S,S*)-**1** and (*R,R*)-**2**, (*S,S*)-**1** dissolution rates are 67.2, 2.9 and 78.7, 12.6 mmol °C^{-1}, respectively (Table 2).

So, the dissolution rates of both the alcohol and the acid component are significantly higher for the heterochiral than for the homochiral gelator combination which suggests that the assemblies in the two systems should be different. Such conclusion is also in accord with observation of different

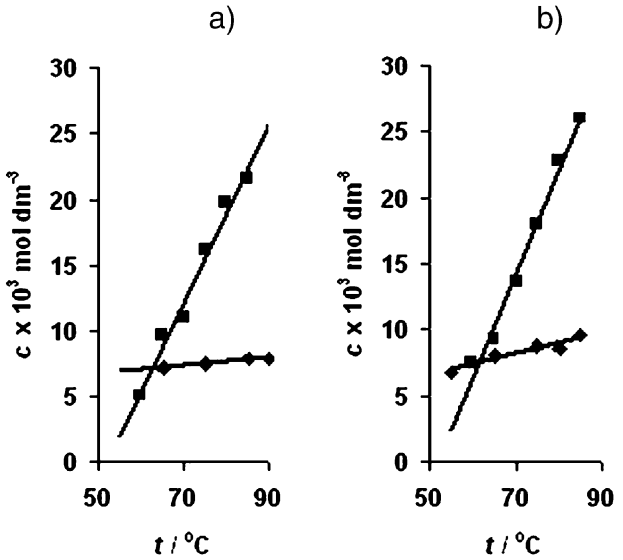

Fig. 6 Gelator concentration increases with increasing temperature in the ^{1}H NMR spectra of (a) (*S,S*)-**1** (◆) + (*S,S*)-**2**(■); (b) (*S,S*)-**1** (◆) + (*R,R*)-**2**(■), toluene gels: $c = c_1 + c_2 = 4.4 \times 10^{-2}$ mol dm^{-3}.

morphologies for homo- and heterochiral toluene gels by TEM and AFM. However, in *o*-xylene gels the dissolution rates for (*S,S*)-**2**, (*R,R*)-**2**, and (*S,S*)-**1** of the homochiral and hereochiral mixtures are practically identical (Table 2 and Supp. Inf. Fig. 4†). This again stands in accord with the TEM observation of similar gel morphologies for the homo- and heterochiral combination, which is reflected in similar component dissolution rates for both combinations of the gelators.

In the ^{1}H NMR spectrum of the (*S,S*)-**1** + *rac*-**2** toluene-d_8 gel, the (*S,S*)-**2**- and (*R,R*)-**2**-NHs are clearly non-equivalent, appearing at δ 7.89 and 7.70 ppm respectively (Fig. 7).

Heating of the gel sample leads to disaggregation of the assemblies and the two signals of the non-equivalent *rac*-**2** NHs practically merge into a single one (Fig. 7), showing that upon disaggregation the NHs have become almost equivalent. The temperature induced changes are fully reversible and cooling of the sample restores the starting NMR spectrum. These results clearly show that the non-equivalency of the (*S,S*)-**2** and (*R,R*)-**2** NHs must be a consequence of their interaction with (*S,S*)-**1**, resulting in diasteroisomerism at the supramolecular level. Hence, different morphologies and temperature–dissolution profiles observed for (*S,S*)-**1** + (*S,S*)-**2**

Table 2 Dissolution slopes (mmol °C^{-1}) of the components of the (*S,S*)-**1** + (*S,S*)-**2** and (*S,S*)-**1** + (*R,R*)-**2** mixed toluene and *o*-xylene gels and the single component (*S,S*)-**1**– and (*S,S*)-**2**–toluene gels

	(*S,S*)-**1** + (*S,S*)-**2**		(*S,S*)-**1** + (*R,R*)-**2**	
	(*S,S*)-**1**	(*S,S*)-**2**	(*S,S*)-**1**	(*R,R*)-**2**
Toluene	2.9	67.2	12.6	78.7
o-Xylene	12.1	44.5	11.6	44.8

	(*S,S*)-**1**	(*S,S*)-**2**		
Toluene	13.5	35.3	—	—

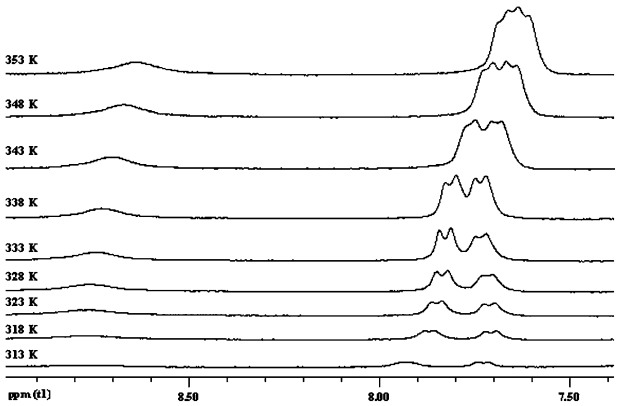

Fig. 7 The temperature induced changes of the chemical shifts of the (*S*,*S*)-**1** NH (δ 8.5–8.6 ppm) and the two nonequivalent *rac*-**2** NHs (δ 7.6–7.95 ppm) in the toluene-d_8 gel of the (*S*,*S*)-**1** + *rac*-**2** 1 : 1 molar mixture.

and (*S*,*S*)-**1** + (*R*,*R*)-**2** toluene gels should be the result of diastereomeric assemblies existing in these systems at the certain level of supramolecular organisation. However, not only in the spectra of the (*S*,*S*)-**1** + (*S*,*S*)-**2** and (*S*,*S*)-**1** + (*R*,*R*)-**2** toluene gels exhibiting distinct morphologies and SGE, but also in the spectra of the *o*-xylene gels showing very similar morphologies, the chemical shifts of the enantiomeric alcohol NHs are different (Supp. Inf. Fig. 5†). The latter observation suggests that formation of diastereoisomeric (*S*,*S*)-**1**–(*S*,*S*)-**2** and (*S*,*S*)-**1**–(*R*,*R*)-**2** assemblies also occurs in *o*-xylene, which, however, do not result in different morphologies, different temperature–dissolution profiles and observation of SGE. These results bring into focus the specific solvation properties of gelled solvent and its specific interactions with gel assemblies, which in certain cases (toluene and *m*- and *p*-xylene) result in significantly different solvation of diastereomeric assemblies and leads to different gel morphology, while in other solvents (benzene and *o*-xylene) both diastereomeric assemblies are similarly solvated, which results in similar morphology and absence of SGE's.

Phase diagrams and thermodynamic parameters for gel melting processes

The difference in the thermally induced dissolution behavior of toluene (*S*,*S*)-**1** + (*S*,*S*)-**2** and (*S*,*S*)-**1** + (*R*,*R*)-**2** gels observed by ^{1}H NMR is also found in their phase transition diagrams (Fig. 8a).

The gel melting temperature (T_g) *vs.* $c_1 + c_2$ (the sum of the component concentrations) curves are distinctly different for (*S*,*S*)-**1** + (*S*,*S*)-**2** and (*S*,*S*)-**1** + (*R*,*R*)-**2** toluene gels (Fig. 8a) and the difference in T_g increases with increasing concentration. The results show that the latter gel is thermally less stable than the former. The phase diagrams obtained for the *o*-xylene gels (Fig. 8b) show less different curves, being almost parallel in contrast to those in the first diagram, also in *o*-xylene, the heterochiral combination gives a thermally less stable gel than the homochiral combination.

The thermodynamic parameters ΔH° and ΔS° can be calculated using gel melting temperatures T_g and molar fractions

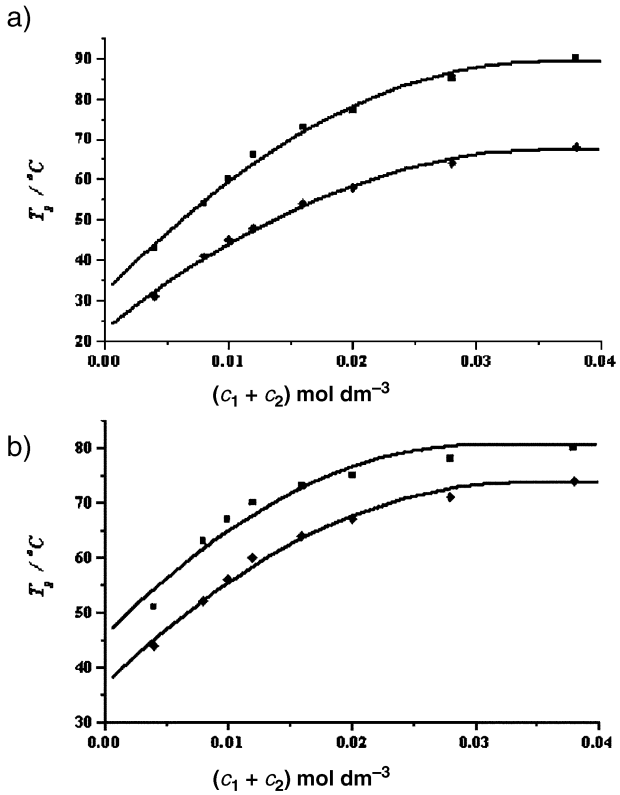

Fig. 8 Phase transition diagrams of (*S*,*S*)-**1** + (*S*,*S*)-**2** (■), (*S*,*S*)-**1** + (*R*,*R*)-**2** (◆) toluene (a) and *o*-xylene (b) gels.

$x_{1,2}$ ($x_{1,2} = n_1 + n_2/n_1 + n_2 + n'$ where n_1 and n_2 are the amounts of components **1** and **2** and n' is the amount of the solvent. Since $n_1 + n_2 \ll n'$, $x_{1,2} = n_1 + n_2/n'$) according to eqn (1).[23]

$$\ln x_{1,2} = -\Delta H^\circ/R \times 1/T_g + \Delta S^\circ/R \qquad (1)$$

The ΔH° and ΔS° values for the toluene and *o*-xylene gel melting processes, calculated from the linear ln $x_{1,2}$ *vs.* $1/T$ plots (Fig. 9), are collected in Table 3.

The free energy changes (ΔG°) for the gel melting processes of the two-component and mono-component toluene and *o*-xylene gels give close values, indicating a similar stability of the gels. However, the enthalpy and entropy changes for the composite gels significantly differ from the sum of the enthalpy and entropy changes for mono-component gels, which strongly suggests that interactions between the components occur in the former systems.

Comparison of the enthalpy and entropy differences for the homochiral and heterochiral gelator combinations of toluene and *o*-xylene gels show that the differences for toluene gels are almost twice as large as those calculated for the *o*-xylene gels: $\Delta(\Delta H^\circ)$ 7.4 kJ mol^{-1} toluene; $\Delta(\Delta H^\circ)$ 3.5 kJ mol^{-1} *o*-xylene and $\Delta(\Delta S^\circ)$ 29.6 J K^{-1} mol^{-1} toluene; $\Delta(\Delta S^\circ)$ 15.6 J K^{-1} mol^{-1} *o*-xylene. The somewhat larger energy difference between the homochiral and heterochiral assemblies of toluene gels suggests their different supramolecular organization. However, the difference between the enthalpy changes for the homochiral (*S*,*S*)-**1** + (*S*,*S*)-**2** and the heterochiral (*S*,*S*)-**1** + (*R*,*R*)-**2** toluene combinations is rather small [$\Delta(\Delta H^\circ)$

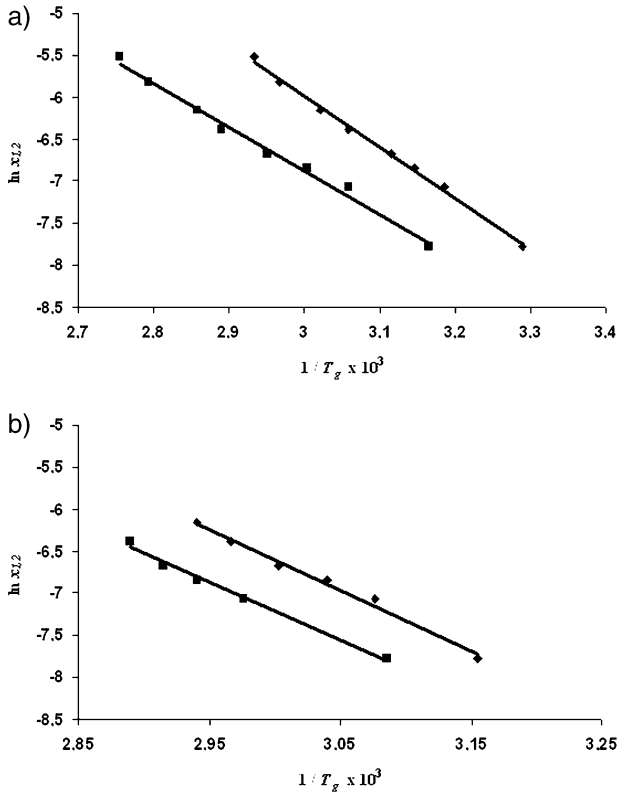

Fig. 9 Plots of ln $x_{1,2}$ *vs.* $1/T_g$ for the (*S*,*S*)-**1** + (*S*,*S*)-**2** (■) and (S,*S*)-**1** + (*R*,*R*)-**2** (◆) toluene (a) and *o*-xylene (b) gels ($r^2 > 0.9$).

7.4 kJ mol^{-1}]. This suggests that the difference in supramolecular organization is not a consequence of different organization involving strong intermolecular interactions, such as hydrogen bonding between oxalamide units or polar carboxylic acid or hydroxyl groups of the gelator molecules, but that it is more likely a consequence of different interactions involving weaker van der Waals interactions between the aggregates or between the aggregates and solvent molecules.

X-Ray powder diffraction (XRPD) of xerogels

As previously reported, the crystal structure of (*S*,*S*)-**2** shows bilayered organization and the XRPD's of both the ground single crystals and the xerogel prepared from toluene show identical major diffraction peaks at 2Θ 5.7, 11.4, 17.1 and 22.8° having the periodicity characteristic of a lamellar organization.[21c] The *d* spacing of 15.5 Å at 2Θ of 5.7° corresponds to the thickness of the (*S*,*S*)-**2** bilayer found in the crystal structure. Thus, in toluene gel, (*S*,*S*)-**2** is organized in the reversed bilayers. The tendency of (*S*,*S*)-**1** to form reversed bilayers in lipophilic solvents was strongly suggested by the results of previous ^{1}H NMR studies.[10a] The XRD of the (*S*,*S*)-**1** xerogel prepared from toluene gel shows the most intensive peaks at low angles (2Θ 4.8, 8.5 and 9.7°), corresponding to *d* spacings of 18.3, 10.4 and 9.0 (Fig. 10a), the appearance of the broad band in the wide-angle region could be a consequence of the slightly disordered structure of the organogel.[24]

The fully minimized conformation of (*S*,*S*)-**1** was generated by molecular modeling using a systematic conformational search and the dimer with mutually hydrogen bonded carboxylic groups as the minimal fragment of a reversed bilayer was constructed. The thickness of the bilayer measured from the CPK model is 18.2 Å and the distance between oxalamide planes gives the value of 10.4 Å (Supp. Inf. Fig. 6†), thus both values nicely correspond to *d* spacings calculated for the two most intensive peaks in the XRD diagram (Fig. 10a).

The diffraction diagram of the (*S*,*S*)-**1** + (*S*,*S*)-**2** xerogel prepared from the toluene gel is shown in Fig. 10b. The diagram clearly represents the sum of (*S*,*S*)-**1** and (*S*,*S*)-**2** diffraction diagrams containing peaks of both components. This shows that the bilayers of each component are simultaneously present in the toluene gel.

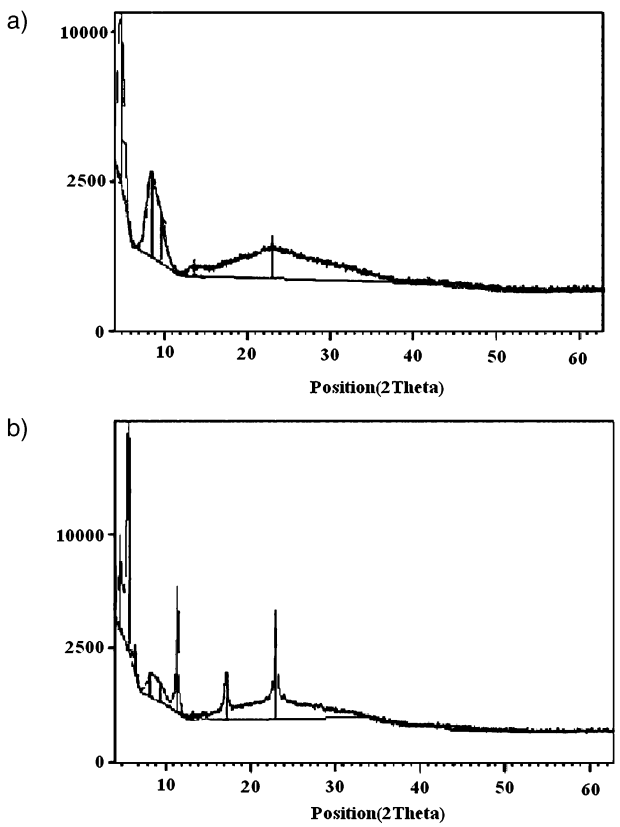

Fig. 10 X-ray powder patterns of xerogels prepared from the toluene gels of (a) (*S*,*S*)-**1** and (b) (*S*,*S*)-**1** + (*S*,*S*)-**2**. The diagram (b) contains the diffraction peaks of (*S*,*S*)-**1** and (*S*,*S*)-**2** at 2Θ of 4.8 and 8.5° and 5.7, 11.4, 17.1 and 22.8°, respectively, indicating the simultaneous presence of bilayers of both components in the (*S*,*S*)-**1** + (*S*,*S*)-**2** toluene gel.

Table 3 Thermodynamic parameters (ΔH°/kJ mol^{-1}and ΔS°/J K^{-1} mol^{-1})[a] obtained from the ln $x_{1,2}$ *vs.* $1/T_g$ plots and calculated free energy changes (ΔG° at 300 K/kJ mol^{-1}) of the two-component (*S*,*S*)-**1** + (*S*,*S*)-**2**, (*S*,*S*)-**1** + (*R*,*R*)-**2** and mono-component (*S*,*S*)-**1** and (*S*,*S*)-**2** toluene and *o*-xylene gels

	Toluene			*o*-Xylene		
	ΔH°	ΔS°	ΔG°	ΔH°	ΔS°	ΔG°
(*S*,*S*)-**1** + (*S*,*S*)-**2**	+43.2	+72.4	+21.5	+56.7	+110.2	+23.6
(*S*,*S*)-**1** + (*R*,*R*)-**2**	+50.6	+102.0	+20.0	+60.2	+125.8	+22.5
(*S*,*S*)-**1**	+54.5	+110.0	+21.5	+57.1	+112.7	+23.3
(*S*,*S*)-**2**	+89.0	+207.5	+26.8	+85.9	+201.2	+25.5

[a] Accuracy on ΔH° and ΔS° is ±10%.

Discussion

To explain the observed SGE effects, the experimental results are interpreted in relation to the possible assembly motifs between (*S,S*)-**1** and (*S,S*)-**2** and (*S,S*)-**1** and (*R,R*)-**2** at different levels of organization: particularly, a possible stereochemical influence on the assembly of the component gelators at the primary, and at higher levels of organization found to exist in gel, is considered.[1b]

At least four levels of organization (**I–IV**) could be anticipated for these types of gelators: the primary level (**I**), resulting from the unidirectional and cooperative intermolecular hydrogen bonding between self-complementary oxalamide units; the secondary level (**II**), comprising from bilayered aggregates; the tertiary level (**III**), comprising unit fibers composed of interacting bilayers; and the quaternary level (**IV**), consisting of bundles of different size formed by interactions between unit fibers (Fig. 11).

At the primary level (**I**), the intermolecular oxalamide–oxalamide hydrogen bonding between homochiral (*S,S*)-**1** and (*S,S*)-**2** gives assemblies with clearly separated lipophilic and polar parts, resembling ampiphilic aggregates and hence favoring formation of reversed bilayers (level **II**) in the lipophilic solvents (Fig. 12a).

It should be noted that such hydrogen bonding between heterochiral (*S,S*)-**1** and (*R,R*)-**2**, would give the primary assemblies with alternating positions of lipophilic and polar parts, which can not form bilayers (Fig. 12b and *vi*). At the secondary level (**II**), the hybrid bilayers consisting of hydrogen bonded (*S,S*)-**1** and (*S,S*)-**2** (Fig. 12, *i*) or those built up from (*S,S*)-**1** and (*S,S*)-**2** (*ii*) or (*S,S*)-**1** and (*R,R*)-**2** (*v*) primary assemblies may form. If any of the hybrid bilayers (*i*), (*ii*) or (*v*) would form, the thermally induced disaggregation would give smaller, NMR observable aggregates consisting of equal proportions of both components; in other words the NMR signals of **1** and **2** would show similar increases in intensity with increasing temperature. The NMR dissolution profiles (Fig. 6) clearly show that this is not the case in any of the toluene and *o*-xylene gels, since the alcohol component **2** in each case gives much higher dissolution slopes than the acid component **1**. Thus, formation of hybrid bilayers (*i*), (*ii*) or (*v*) can be ruled out on the basis of the dissolution profiles.

If the bilayers of a single component form (Fig. 12, *iii* and *vii*) that subsequently organize into separated unit fibers of each component, the thermally induced disassembly should

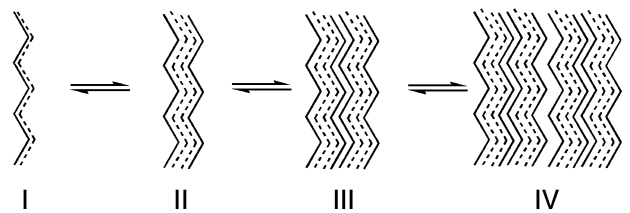

Fig. 11 Levels of organization in gels: primary assemblies (**I**) formed by unidirectional hydrogen-bonding between oxalamide units of gelator molecules; the secondary level of organization (**II**) of reversed bilayers formed by primary assemblies; the tertiary level (**III**) giving unit fibers by lipophilic interactions between bilayers; and the quaternary level (**IV**) of bundles formed by the interacting unit fibers.

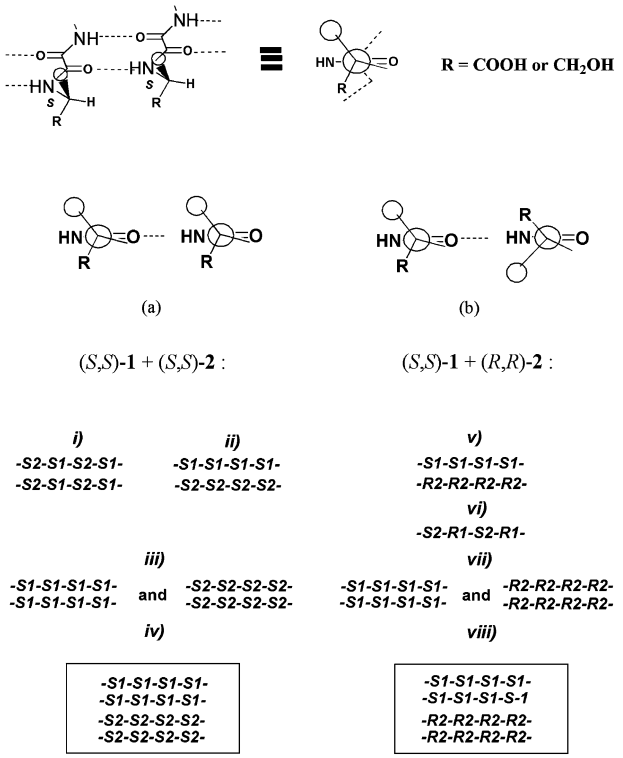

Fig. 12 Possible organization motifs of the (*S,S*)-**1**, (*S,S*)-**2** and (*R,R*)-**2** components (abbreviated as ***S*1**, ***S*2** and ***R*2**) in toluene gels into hybrid bilayers (*i*, *ii* and *v*), a monolayer assembly (*vi*), the separated unit fibers, each containing single component bilayers (*iii* and *vii*), and the composite unit fibers formed by interacting bilayers of the components **1** and **2** (*iv* and *viii*).

give the NMR observable (*S,S*)-**1** and (*S,S*)-**2** (or (*R,R*)-**2**) aggregates in different proportions depending on the solubility of the components. In such a case, two independent gel networks would coexist and the maximal volumes of the solvent gelled by the (*S,S*)-**1** + (*S,S*)-**2** and (*S,S*)-**1** + (*R,R*)-**2** mixtures should be the same. In other words, no synergism could be observed in such a case and also, the chemical shifts of the (*S,S*)-**2** and (*R,R*)-**2** NHs should appear identical in the NMR spectra of (*S,S*)-**1** + (*S,S*)-**2** and (*S,S*)-**1** + (*R,R*)-**2** gels. Since chiral synergism is observed for the (*S,S*)-**1** + (*S,S*)-**2**/(*S,S*)-**1** + (*R,R*)-**2** toluene gels, and the (*S,S*)-**2** and (*R,R*)-**2** NHs give distinct signals in the ^{1}H NMR spectra of the (*S,S*)-**1** + *rac*-**2** toluene and *o*-xylene gels, organizations *iii* and *vii* can be ruled out as well.

At the tertiary level of organization (Fig. 11, **III**), the (*S,S*)-**1** and (*S,S*)-**2** (Fig. 12, *iv*) and also (*S,S*)-**1** and (*R,R*)-**2** (Fig. 12, *viii*) bilayer aggregates may interact, giving unit fibers containing both components: bilayer organizations *iv* and *viii* are diastereomeric and hence the unit fibers must also be different. This should result in different gelation efficiency and non-equivalency of the (*S,S*)-**2** and (*R,R*)-**2** NHs in the NMR spectra of their aggregates with (*S,S*)-**1**. The dissolution slopes in this case should give different values for **1** and **2**, depending on the stability of each single component bilayer. This type of organization is in accord with all of the provided experimental results. The thermodynamic parameters (Table 3) show a small enthalpy difference between the homochiral and heterochiral

gels. It appears that much weaker supramolecular interactions, such as lipophilic interactions that occur between interacting reversed bilayers must be responsible for the observed synergism. The non-equivalency of the (*S*,*S*)-**2** and (*R*,*R*)-**2** NHs as observed in the NMR spectra of gels with *rac*-**2** component (Fig. 7 and Supp. Inf.†) strongly suggest interaction of the component bilayers which results in induced diastereoisomerism at the tertiary level of organization.

As shown schematically in Fig. 13, different directionality of oxalamide hydrogen bonding occurs in the interacting (*S*,*S*)-**1**–(*S*,*S*)-**2** and (*S*,*S*)-**1**–(*R*,*R*)-**2** bilayers, making (*S*,*S*)-**2** and (*R*,*R*)-**2** NHs non-equivalent in such aggregates.

The XRPD of xerogels should give diffraction peaks corresponding to both present bilayers, which indeed have been observed (Fig. 10). However, the lipophilic interactions between the bilayers in the unit fibers appear different (Fig. 13) due to different orientation of *i*-Bu groups in the (*S*,*S*)-**1**–(*S*,*S*)-**2** and (*S*,*S*)-**1**–(*R*,*R*)-**2** bilayer aggregates. This may give different packing of (*S*,*S*)-**1**–(*S*,*S*)-**2** and (*S*,*S*)-**1**–(*R*,*R*)-**2** bilayers in the unit fibers and also result in different solvation of such fibers by the same solvent. TEM and AFM investigations (Fig. 3) revealed different gel morphologies for homo- and hetero-chiral gelator combinations: formation of thin fibers in the (*S*,*S*)-**1** + (*S*,*S*)-**2** toluene, *p*- and *m*-xylene gels and thick and straight fiber bundles in the (*S*,*S*)-**1** + (*R*,*R*)-**2** gels with the same solvents. Apparently, toluene, and *m*- and *p*-xylene are capable of providing highly specific interactions with diastereomeric gel assemblies, which result in different gel morphologies. However, benzene and *o*-xylene are not capable of specific solvation of diasteromeric assemblies and the properties and morphologies of homo- and heterochiral gels are similar. The highly important role of the organic solvent in determining the gel properties and its direct participation in the formation of fibers was recently revealed by the AFM study of the gels of cholesterol–stilbene gelators.[25] The results clearly prove strong gel fiber–solvent interactions and participation of the solvent molecules in the formation of both unit fibers and fiber bundles.

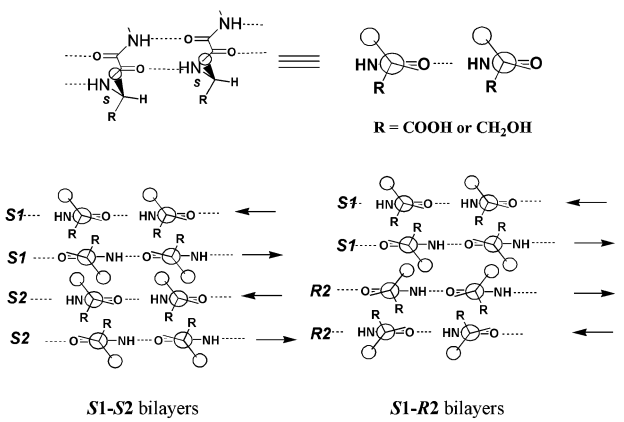

Fig. 13 Interactions between the (*S*,*S*)-**1**–(*S*,*S*)-**2** and (*S*,*S*)-**1**–(*R*,*R*)-**2** bilayers lead to diasteromerism at the supramolecular level. Different directionality of NH···O=< hydrogen bonding, indicated by arrows, results in the non-equivalence of the (*S*,*S*)-**2** and (*R*,*R*)-**2** NHs in the ^{1}H NMR spectra of the two aggregate systems.

Conclusion

We report on the observation of the synergic gelation effect (SGE) in two-component gels, which shows that the defined mass of the equimolar mixture of two constitutionally different gelators is capable to gel an impressively larger volume of certain solvents than the equal mass of each of the single components and that the weighted amount of the homochiral (*S*,*S*)-**1** + (*S*,*S*)-**2** equimolar mixture is capable to gel up to 5 times larger volume of the same solvent than the equal mass of the heterochiral (*S*,*S*)-**1** + (*R*,*R*)-**2** or the (*S*,*S*)-**1** + *rac*-**2** equimolar mixture. We provide the evidence that synergism depends on chirality of the component gelators and on the solvent properties. Formation of composite gels assemblies from constitutionally different gelator molecules can be considered as the supramolecular variant of molecular co-polymerization. It should be noted that in our systems at lower organizational levels (**I** and **II**, Fig. 11) both components give self-assembled aggregates and that the co-assembly exemplified by lipophilic interactions between the single component reversed bilayers occurs only at the **III** and **IV** levels of organization. We believe that the presented results shed more light on the supramolecular co-assembly in gels and may endow the preparation of more complex systems with improved properties based on mixtures of constitutionally and stereochemically different gelator molecules.

Experimental

Compounds **1** and **2** were prepared following procedures described previously.[21a,c]

Gelation experiments

A weighted amount of compound **1** or **2** or their 1 : 1 molar mixture was placed in a test tube and measured volumes (100–500 μL) of a selected solvent were repeatedly added. After each addition, the mixture was heated until the substance dissolved, then allowed to cool spontaneously to room temperature, and gel formation was checked by test tube inversion. The procedure was repeated until the sample fluidity was restored at room temperature.

^{1}H NMR experiments

All ^{1}H NMR experiments were done on a Bruker AV-300 spectrometer. The temperature dependent ^{1}H NMR spectra of **1** and **2** toluene-d_8 and *o*-xylene-d_{10} gels (V = 0.65 mL; c_1 + c_2 = 0.044 mol dm^{-3}) were recorded at different temperatures by raising the temperature by 5 °C from 25–80 °C in the presence of a known concentration of 1,1,2,2-tetrachloroethane, used as an internal standard.

Phase transition temperature measurements

Gelation temperatures (T_g) were determined by the inverse flow method. The test tube that contained gel was immersed inversely in a thermostated water bath. The temperature was raised at a rate of 0.5 °C min^{-1}. The T_g was defined as the temperature at which the gel turned into the sol phase.

TEM measurements

For transmission electron microscopy, a piece of gel was placed on a carbon-coated copper grid and removed after 1 min, leaving some small patches of the gel on the grid. After samples were dried at low pressure, they were shadowed at an angle of 20° with palladium. The samples were examined with a FEI MORGAGNI 268D transmission electron microscope operating at 70 kV.

Powder X-ray diffraction

The toluene gels of (*S*,*S*)-**1** and (*S*,*S*)-**1** + (*S*,*S*)-**2** mixtures were prepared in a sample tubes and frozen by liquid nitrogen. The frozen specimens were evaporated by a vacuum pump at 0.6 mmHg for 1 day at room temperature. X-ray diffractograms of the xerogels were recorded on X'-PERT Philips 3040 powder diffractometer.

AFM measurements

Atomic Force Microscopy images were recorded under ambient conditions using a Digital Instrument Multimode Nanoscope IIIa operating in the tapping mode regime. AFM samples were prepared by drop casting a dilute solution of nanostructures (5.0 μL of a toluene gels suspended in 0.100 mL toluene) on freshly cleaved mica (Ted Pella).

Acknowledgements

The financial support from the Croatian Ministry of Science, Education and Technology is gratefully acknowledged.

References

1 (*a*) F. Fages, F. Voegtle and M. Žinić, in *Low Molecular Mass Gelators. Design Self-Assembly Function*, ed. F. Fages, Springer-Verlag, Berlin, 2005, pp. 77–131; (*b*) L. A. Estroff and A. D. Hamilton, *Chem. Rev.*, 2004, **104**, 1201–1218; (*c*) O. Gronwald, E. Snip and S. Shinkai, *Curr. Opin. Colloid Interface Sci.*, 2002, **7**, 148–1218; (*d*) J. H. van Esch and B. L. Feringa, *Angew. Chem., Int. Ed.*, 2000, **39**, 2263–2266; (*e*) P. Terech and R. G. Weiss, *Chem. Rev.*, 1997, **97**, 3133–3159.
2 J. van Esch, F. Schoonbeek, M. De Loos, E. M. Veen, R. M. Kellog and B. L. Feringa, *Nato ASI Series C, Mathematical and physical sciences, Vol. 527*, Kluwer Academic Publishers, 1999, pp. 233–259.
3 K. Murata, M. Aoki, T. Suzuki, T. Harada, H. Kawabata, T. Komori, F. Ohseto, K. Ueda and S. Shinkai, *J. Am. Chem. Soc.*, 1994, **116**, 6664–6676.
4 (*a*) J. L. Pozzo, G. Clavier, F. Rustmeyer and H. Bouas-Laurent, *Mol. Cryst. Liq. Cryst.*, 2000, **344**, 101–106; (*b*) J. L. Pozzo, G. Clavier and J. P. Desvergne, *J. Mater. Chem.*, 1998, **8**, 2575–2577.
5 L. Frkanec, M. Jokić, J. Makarević, K. Wolsperger and M. Žinić, *J. Am. Chem. Soc.*, 2002, **124**, 9716–9717.
6 (*a*) S.-L. Zhou, S. Matsumoto, H.-D. Tian, H. Yamane, A. Ojida, S. Kiyonak and I. Hamachi, *Chem.–Eur. J.*, 2005, **11**, 1130–1136; (*b*) Z. Yang, H. Gu, Y. Zhang, L. Wang and B. Xu, *Chem. Commun.*, 2004, 208–209; (*c*) Y. Zhang, H. Gu, Z. Yang and B. Xu, *J. Am. Chem. Soc.*, 2003, **125**, 13680–13681.
7 (*a*) J. C. Tiller, *Angew. Chem., Int. Ed.*, 2003, **42**, 3072–3075; (*b*) B. Xing, C. W. Yu, K. H. Chow, P. L. Ho, D. Fu and B. Xu, *J. Am. Chem. Soc.*, 2002, **124**, 14846–14847.
8 K. Y Lee and D. J. Mooney, *Chem. Rev.*, 2001, **101**, 1869–1880.
9 S. Kiyonaka, K. Sugiyasu, S. Shinkai and I. Hamachi, *J. Am. Chem. Soc.*, 2002, **124**, 10954–10955.
10 (*a*) K. J. C. van Bommel, A. Friggeri and S. Shinkai, *Angew. Chem., Int. Ed.*, 2003, **42**, 980–999; (*b*) J. H. Jung, S.-H. Lee, J.-S. Yoo, K. Yoshida, T. Shimizu and S. Shinkai, *Chem.–Eur. J.*, 2003, **9**, 5307–5313; (*c*) J. H. Jung, S. Shinkai and T. Shimizu, *Nano Lett.*, 2002, **2**, 17–20; (*d*) K. J. C. van Bommel and S. Shinkai, *Langmuir*, 2002, **18**, 4544–4548.
11 (*a*) M. Barboiu, S. Cerneaux, A. van der Lee and G. Vaughan, *J. Am. Chem. Soc.*, 2004, **126**, 3545–3550; (*b*) S. Kobayashi, N. Hamasaki, M. Suzuki, M. Kimura, H. Shirai and K. Hanabusa, *J. Am. Chem. Soc.*, 2002, **124**, 6550–6551.
12 (*a*) A. Heeres, C. van der Pol, M. Stuart, A. Friggeri, B. L. Feringa and J. van Esch, *J. Am. Chem. Soc.*, 2003, **125**, 14252–14253; (*b*) M. de Loos, J. van Esch, R. M. Kellog and B. L. Feringa, *Angew. Chem., Int. Ed.*, 2001, **40**, 613–616; (*c*) J. van Esch, S. De Feyter, R. M. Kellog, F. De Schryver and B. L. Feringa, *Chem.–Eur. J.*, 1997, **3**, 1238–1243.
13 G. Meiden-Gundert, L. Klein, M. Fischer, F. Vögtle, K. Heuze, J.-L. Pozzo, M. Vallier and F. Fages, *Angew. Chem., Int. Ed.* 2001, **40**, 3164–3166.
14 (*a*) K. Hanabusa, Y. Matsumoto, T. Miki, T. Koyama and H. Shirai, *J. Chem. Soc., Chem. Commun.*, 1994, 1401–1402; (*b*) K. Hanabusa, M. Yamada, M. Kimura and H. Shirai, *Angew. Chem., Int. Ed. Engl.*, 1996, **35**, 1949–1951.
15 (*a*) J. J. D. de Jong, P. R. Hania, A. Pugžlys, L. N. Lucas, M. de Loos, R. M. Kellogg, B. L. Feringa, K. Duppen and J. H. van Esch, *Angew. Chem., Int. Ed.*, 2005, **44**, 2373–2376; (*b*) K. J. C. van Bommel, C. van der Pol, I. Muizebelt, A. Friggeri, A. Heeres, A. Meetsma, B. L. Feringa and J. van Esch, *Angew. Chem., Int. Ed.*, 2004, **43**, 1663–1667.
16 (*a*) M. Shirakawa, N. Fujita and S. Shinkai, *J. Am. Chem. Soc.*, 2005, **127**, 4164–4165; (*b*) S. Kawano, N. Fujita and S. Shinkai, *Chem.–Eur. J.*, 2005, **11**, 4735–4742; (*c*) K. Sugiyasu, N. Fujita and S. Shinkai, *Angew. Chem., Int. Ed.*, 2004, **43**, 1229–1233; (*d*) S. Kiyonaka, S. Shinkai and H. Hamachi, *Chem.–Eur. J.*, 2003, **9**, 976–983.
17 T. Sumiyoshi, K. Nishimura, M. Nakano, T. Handa, Y. Miwa and K. Tomioka, *J. Am. Chem. Soc.*, 2003, **125**, 12137–12142.
18 (*a*) T. Naota and H. Koori, *J. Am. Chem. Soc.*, 2005, **127**, 9324–9325; (*b*) N. Mohmeyer and H.-W. Schmidt, *Chem.–Eur. J.*, 2005, **11**, 863–872; (*c*) M. George, G. Tan, V. T. John and R. G. Weiss, *Chem.–Eur. J.*, 2005, **11**, 3243–3254; (*d*) G. Buhler, M. C. Feiters, R. J. M. Nolte and K. H. Dotz, *Angew. Chem., Int. Ed.*, 2003, **42**, 2494–2497.
19 (*a*) M. Suzuki, T. Sato, A. Kurose, H. Shirai and K. Hanabusa, *Tetrahedron Lett.*, 2005, **46**, 2741–2745; (*b*) M. Suzuki, M. Yumoto, M. Kimura, H. Shirai and K. Hanabusa, *Chem.–Eur. J.*, 2003, **9**, 348–354.
20 (*a*) B. Huang, A. R. Hirst, D. K. Smith, V. Castelleto and I. W. Hamley, *J. Am. Chem. Soc.*, 2005, **127**, 5901–5910; (*b*) A. R. Hirst, D. K. Smith, M. C. Feiters and H. P. M. Geurts, *Chem.–Eur. J.*, 2004, **10**, 1922–1932; (*c*) P. Babu, N. M. Sangeetha, P. Vijaykumar, U. Maitra, K. Rissanen and A. R. Raju, *Chem.–Eur. J.*, 2003, **9**, 1922–1932; (*d*) A. Friggeri, O. Gronwald, K. J. C. van Bommel, S. Shinkai and D. N. Reinhoudt, *J. Am. Chem. Soc.*, 2002, **124**, 10754–10758; (*e*) K. S. Partridge, D. K. Smith, G. M. Dykes and P. T. McGrail, *Chem. Commun.*, 2001, 319–320; (*f*) S. W. Jeong, K. Murata and S. Shinkai, *Supramol. Sci.*, 1996, **3**, 83–86; (*g*) K. Hanabusa, T. Miki, Y. Taguchi, T. Koyama and H. Shirai, *J. Chem. Soc., Chem. Commun.*, 1993, 1382–1384.
21 (*a*) J. Makarević, M. Jokić, Z. Raza, Z. Štefanić, B. Kojić-Prodić and M. Žinić, *Chem.–Eur. J.*, 2003, **9**, 5567–5580; (*b*) J. Makarević, M. Jokić, L. Frkanec, D. Katalenić and M. Žinić, *Chem. Commun.*, 2002, 2238–2239; (*c*) J. Makarević, M. Jokić, B. Perić, V. Tomišić, B. Kojić-Prodić and M. Žinić, *Chem.–Eur. J.*, 2001, **7**, 3328–3341.
22 (*a*) D. C. Duncan and D. G. Whitten, *Langmuir*, 2000, **16**, 6445–6452; (*b*) F. Menger, Y. Yamasaki, K. K. Catlin and T. Nishimi, *Angew. Chem.*, 1995, **107**, 616–618 (*Angew. Chem., Int. Ed. Engl.*, 1995, **34**, 585–586).
23 J.-P. Desvergne, T. Brotin, D. Meerschaut, G. Clavier, F. Placin, J.-L. Pozzo and H. Bousa-Laurent, *New J. Chem.*, 2004, **28**, 234–243.
24 (*a*) M. George, S. L. Snyder, P. Terech, C. Glinka and R. G. Weiss, *J. Am. Chem. Soc.*, 2003, **125**, 10275–10283; (*b*) J. H. Jung, S. Shinkai and T. Shimizu, *Chem.–Eur. J.*, 2002, **8**, 2684–2690.
25 R. Wang, C. Geiger, L. Chen, B. Swanson and D. G. Whitten, *J. Am. Chem. Soc.*, 2000, **122**, 2399–2400.